Frontiers of Information Technology & Electronic Engineering
www.jzus.zju.edu.cn; engineering.cae.cn; www.springerlink.com
ISSN 2095-9184 (print); ISSN 2095-9230 (online)
E-mail: jzus@zju.edu.cn

Aircraft safety analysis based on differential manifold theory and bifurcation method*

Chi ZHOU†, Ying-hui LI, Wu-ji ZHENG, Peng-wei WU

School of Aeronautics and Astronautics Engineering, Air Force Engineering University, Xi'an 710038, China

†E-mail: 15279122641@163.com

Received July 1, 2017; Revision accepted Sept. 13, 2017; Crosschecked Jan. 22, 2019

Abstract: Loss of control (LOC) is considered one of the leading causes of fatal aircraft accidents worldwide. Reducing LOC is critical to improve flight safety. Although it is still vaguely defined, LOC is generally associated with a flight state that is outside the safety envelope, with nonlinear influences of aircraft dynamics and incorrect handling by the flight crew. We have studied how nonlinear factors and pilot operations contribute to LOC. In this study, the stall point and bifurcation point are confirmed using the bifurcation analysis, and the results show that the aircraft will stall when excessive elevator movement is commanded. Moreover, even though there may be an equilibrium state in one of the elevator deflections, the flight state may still be outside the flight safety envelope. When the flight state is near the edge of the flight safety envelope, the strategy to regulate the elevator deflection is super-sensitive, and a slight change in the elevator deflection may contribute to a flight state outside the safety envelope. To solve this issue, the differential manifold theory is introduced to determine the safety envelope. Examples are provided using NASA's generic transport model.

Key words: Loss of control; Safety envelope; Aircraft dynamic; Bifurcation analysis; Differential manifold theory
https://doi.org/10.1631/FITEE.1700435 **CLC number:** V328

1 Introduction

With the frequency of commercial air travel on the rise, it has become increasingly important to improve the safety of current and future aircraft operation in the national airspace system. According to the statistics of accident reports available on the aviation safety network website, 59% of fatal aircraft accidents occurring between 1997 and 2006 were associated with loss of control (LOC) (Ranter, 2007). LOC is considered one of the leading contributors to aircraft accidents (Zhang et al., 2016), as a result of aircraft exceeding the flight safety envelope. Many of these cases have not been realized by the flight crew (Klyde and McRuer, 2009). Klyde and McRuer (2009) noted that LOC was connected with a flight state outside the flight safety envelope. However, they only noted how to identify LOC in upset conditions and did not provide direct links between LOC and the aircraft dynamic system. Thus, their study could not be used proactively to identify the weaknesses or limitations in the aircraft. When an aircraft encounters upset conditions, such as aging of the airframe, environmental disturbances, degraded flight operations, and aerodynamic upsets, the flight envelope may be greatly affected and the flight control system can provide the flight crew with incorrect control instructions. Therefore, unaware of these upset conditions, the flight system may operate under a conflicting envelope. This has been emphasized by a number of high-profile accidents such as the ATR72-212 accident in 1994, which was caused by ice accretion. In this accident, the plane had been operating in violation of the flight safety envelope.

* Project supported by the National Basic Research Program (973) of China (No. 2015CB755805) and the National Natural Science Foundation of China (No. 61374145)
ORCID: Chi ZHOU, http://orcid.org/0000-0002-5088-3919

The roll occurred anomaly at an angle of attack of 5°, which is much lower than the angle of attack limit (18.1°) under normal conditions (Merret et al., 2002).

For all aircrafts, once the flight control laws are determined, the entire dynamic system is fixed. It means that there is a limitation on the deflection of the elevators. Once the control laws are maintained constantly, the system will not be able to return to its original equilibrium or even cause LOC when the elevator deflections exceed the limitation. To solve this issue, the bifurcation analysis is used to study elevator deflections and how they change the trim state of the aircraft. It is widely known that the bifurcation analysis method can help understanding the flight mechanics in upset conditions (Sieber and Krauskopf, 2008; Xin and Shi, 2015). Therefore, it will be helpful in guiding operation, reducing the accidents attributed to LOC along with the loss of life and the large financial costs (Khatri and Sinha, 2011; Engelbrecht et al., 2012). Engelbrecht et al. (2012) noted that the stability of the system was associated with the bifurcation point. In excessive elevator deflections, bifurcation will occur and the system will be unstable. However, the bifurcation point identifies only the limitation of the elevator deflections and will fail if applied to a neighboring region (Kwatny et al., 2013). It means that if the flight state is near the boundary of the flight safety envelope, the strategy to regulate elevator deflections is super-sensitive. A slight change in elevator deflections may contribute to a flight state outside the safety envelope or even lead to LOC. To improve the flight safety and reduce the accidents caused by LOC, a reliable method to assess the flight safety envelope should be established in real time.

For conventional envelope protection, the flight safety envelope is defined as the range of airspeed, flight altitude, and normal load factors, at which the aircraft can operate safely (Sharma et al., 2004). It means that the flight envelope protection is meant to apply limitations and the flight state should not exceed these limitations. However, the conventional method to define the flight envelope cannot consider upset conditions, such as a change in flight dynamics. Hence, the conventional envelope methods, which use predetermined limitations for parameters such as the angle of attack and bank angle, are no longer effective in icing conditions. Thus, it is important to introduce the concept of changing conditions that are dependent on weather conditions and dynamically enforced to ensure the flight safety.

Consideration of more conditions that affect the flight envelope is a problem that has been studied by many researchers. One method to compute the safety envelope is based on reachable set techniques (Lygeros et al., 1999; Bayen et al., 2007; Zuo et al., 2013; Weekly et al., 2014; Goncharova and Ovseevich, 2016). The level set method using the Hamilton-Jacobi (HJ) partial differential equation is generally used to obtain the reachable set. It allows us to predict, to some extent, the states that can be reached with a given control authority from a trim condition. The restricted set of flight states at each key point is seen as the target set. By solving the HJ partial differential equation with the optimal control laws, the largest safe sets can be obtained. The method is based on the optimal control and level set methods. It simultaneously computes a maximum controlled invariant set and a set-valued control law guaranteed to keep the aircraft within a safe set of states under autopilot mode switching. For an aircraft, the reachable set is a safe set, and trajectories from states in the reachable set can reach the target set in the time horizon, subject to some control laws. However, we cannot know which control law can be used to make the state reach the target set. Trajectories from states outside the reachable set cannot reach the target set in any time horizon, subject to any control law. Therefore, it is difficult to combine the reachable set techniques with the method of bifurcation. In addition, another important method using the region of attraction (ROA) method (Haghighatnia and Moghaddam, 2013; Khodadadi et al., 2014) was proposed to analyze the flight safety based on Lyapunov's stability theory (Pandita et al., 2009). The ROA method offers the ability to predict a stable set in the state space around a given equilibrium, in which the system will return to the equilibrium. Although this method can take many conditions into account, it is still fairly conservative and cannot be used in engineering applications.

In this study, a novel method based on the differential manifold theory has been presented to overcome the conservative nature of the flight envelope assessment. The methodology based on the differential manifold theory (Krauskopf and Osinga,

1999; Chaichi et al., 2005; Osinga, 2005) is one method for estimating the stable region in a nonlinear dynamical system, which can be seen as the dynamical envelope for aircraft systems. It is shown that the stability boundary of the nonlinear dynamical system consists of the union of the stable manifolds of all equilibrium points and/or closed orbits on the stability boundary (Chiang et al., 1988). By introducing the differential manifold theory, an accurate flight safety envelope is determined. Thus, the differential manifold theory and the bifurcation analysis method complement each other nicely. To sum up, the two approaches have properties capable of guiding operation and determining the flight safety envelope and the results will be discussed in Section 4.

2 Method for flight safety analysis

Two approaches are introduced for flight safety analysis. The differential manifold theory is used to determine an accurate safe envelope and the bifurcation analysis is used to guide pilot operation.

2.1 Differential manifold theory

A nonlinear autonomous dynamical system can be described by the differential equation:

$$\dot{\boldsymbol{x}} = f(\boldsymbol{x}). \tag{1}$$

The equilibrium point (EP) can be denoted by the solution of the equation $f(\boldsymbol{x})=0$. Suppose none of the eigenvalues of the Jacobian matrix $\boldsymbol{J}_{\boldsymbol{x}}$ at $\boldsymbol{x}$ has zero real part, then the EP $\boldsymbol{x}$ of f is said to be hyperbolic.

For a hyperbolic EP $\boldsymbol{x}$, there are two classes of EP. If all of the eigenvalues of the Jacobian matrix possess only negative real parts, the EP is called the stable equilibrium point (SEP), and the opposite is called the unstable equilibrium point (UEP). For a UEP, if all of the eigenvalues possess positive parts, it is called a source. If not, it is called a saddle.

For a saddle x_0, the eigenvalues that have negative parts are restricted to the stable substance E^{s} and the eigenvalues that have positive parts are restricted to the unstable substance E^{u}. The dimensions of E^{s} and E^{u} are n_{s} and n_{u}, respectively. Obviously, $n_{\mathrm{s}}+n_{\mathrm{u}}=n$. The stable and unstable manifolds $W^{\mathrm{s}}(x_0)$ and $W^{\mathrm{u}}(x_0)$ of x_0 can be defined as follows:

$$W^{\mathrm{s}}(x_0) = \{\boldsymbol{x} | \lim_{t\to\infty} \varphi(t, \boldsymbol{x}) = x_0\}, \tag{2}$$

$$W^{\mathrm{u}}(x_0) = \{\boldsymbol{x} | \lim_{t\to-\infty} \varphi(t, \boldsymbol{x}) = x_0\}, \tag{3}$$

where $\varphi(t, \boldsymbol{x})$ is the flow induced by the vector field f, also known as the trajectory.

For an SEP x_{s}, the stability region $A(x_{\mathrm{s}})$ can be defined as $W^{\mathrm{s}}(x_{\mathrm{s}})$ and its boundary is called the stability boundary, defined by $\partial A(x_{\mathrm{s}})$ with dimension $n-1$. Chiang et al. (1988) noted that the stability region could be determined by the stable manifolds of UEPs that were on the stability boundary of an SEP. The differential manifold theory must satisfy the following conditions: (1) All the UEPs on $\partial A(x_{\mathrm{s}})$ are hyperbolic. (2) The stable and unstable manifolds on $\partial A(x_{\mathrm{s}})$ should satisfy the transversality condition. (3) Every trajectory on $\partial A(x_{\mathrm{s}})$ will approach one of the equilibrium points as $t\to\infty$.

Details of how to determine the stability region are presented. First, for a nonlinear autonomous dynamical system $\dot{\boldsymbol{x}} = f(\boldsymbol{x})$, all the EPs can be determined by solving the equation $f(\boldsymbol{x})=0$. Second, we determine the eigenvalues of the Jacobian matrix $\boldsymbol{J}_{\boldsymbol{x}}$ and identify the SEPs and UEPs. Third, one of the SEPs is used as the operating point to determine all of the UEPs on the stability boundary. Finally, all of the UEPs on the stability boundary are used to determine the stability region by the geodesic circles method (Krauskopf et al., 2005). The flow chart is shown in Fig. 1. Details of the geodesic circles method are as follows:

1. Determine the initial geodesic circle. Let x_i be one of the UEPs on the stability boundary. First, the eigenvectors of x_i are obtained by computing the Jacobian matrix. Second, the stable eigenvectors are transformed to the stable characteristic subspace. Third, an initial geodesic circle is drawn on the characteristic subspace where x_i is the center of the circle and r is the radius. Finally, take N points $\{p_{1,1}, p_{1,2}, \ldots, p_{1,N}\}$ evenly on the circle.

2. Calculate the trajectory. Points $\{p_{1,1}, p_{1,2}, \ldots, p_{1,N}\}$ are used as the initial set of points. The inverse time integration is performed and the calculation stops until the trajectory length reaches the set point L. The first-generation trajectories $\{T_{1,1}, T_{1,2}, \ldots, T_{1,N}\}$ are obtained and their terminal points are recorded as $\{p_{2,1}, p_{2,2}, \ldots, p_{2,N}\}$.

3. Check and readjust the initial set of points. We

first check the distance between the trajectories. If the distance between the two trajectories is greater than D_{max}, a new point will be inserted. Conversely, if the distance is less than D_{min}, one of the points will be deleted. Finally, readjust the initial set of points and return to step 2. Do not go to the next step until the requirements are satisfied.

4. The terminal points determined in step 3 are used as the initial points of the second-generation trajectories. Repeat step 2 until the number of iterations reaches Z_{max}.

5. Connect the trajectories of adjacent generations and form the boundary.

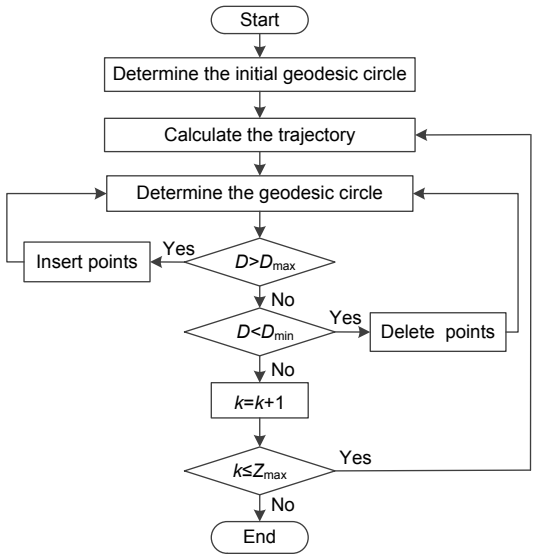

Fig. 1 Flow chart of envelope determination in the geodesic circles method

2.2 Bifurcation analysis theory

The bifurcation analysis method is applied to a nonlinear autonomous dynamical system:

$$\dot{\boldsymbol{x}} = f(\boldsymbol{x}, u), \tag{4}$$

where f is a set of nonlinear differential functions, $\boldsymbol{x}$ is the state vector, and u is a controller input. In bifurcation analysis of state solutions, the one-parameter bifurcation diagram of equilibrium is generated by setting $\dot{\boldsymbol{x}}$ to 0 and solving the resulting simultaneous equations (Jahnke and Culick, 1994). For an aircraft system, the equilibrium point will change when the elevator deflections and controller parameters vary. Hence, the bifurcation analysis method can be used to analyze the influence on equilibrium points of different elevator deflections, and the optimal input can be determined.

3 Dynamic model

Aircraft flight dynamics typically consist of the 8th-order nonlinear equations for rigid body aircraft motion. However, it is difficult for these high-dimensional systems to visualize more than two dimensions of manifolds (Qi et al., 2000). To study them using the NASA's generic transport model (GTM) and identify the attractors that have an effect on the flight dynamic envelope, a two-dimensional manifold is implemented. Furthermore, the effect of flight velocity V_t is considered. The dynamics of the longitudinal are given as follows:

$$\begin{cases} \dot{\alpha}=q+(-L+mg\cos(\alpha-\theta))/(mV_t), \\ \dot{\theta}=q, \\ \dot{q}=M/I_z, \end{cases} \tag{5}$$

$$\begin{cases} L=(F_x+T_x)\sin\alpha-(F_z+T_z)\cos\alpha, \\ M=0.5\rho V_t^2 ScC_m, \\ F_x=0.5\rho V_t^2 SC_x, \\ F_z=0.5\rho V_t^2 SC_z, \end{cases} \tag{6}$$

where α is the angle of attack, θ is the pitch angle, q is the pitch rate, L is the lift of craft, m is the mass, g is the gravity acceleration, M is the aerodynamic moment of the longitudinal, I_z is the moment inertias along the aircraft's z-axis, F_x and F_z are the axial forces of the x- and z-body axes respectively, T_x and T_z are the aircraft thrusts of the x- and z-body axes respectively, ρ is the atmospheric density, S is the reference wing surface area, and c is the mean aerodynamic chord. Because the aircraft dynamic used in this study is GTM, the detailed polynomial model parameters of the pitching moment coefficient C_m, axial force coefficient C_x, and the normal force coefficient C_z can be found in Kwatny et al. (2013).

It is widely known that proportional-integral-derivative (PID) controllers can be used to improve the quality of an aircraft. Hence, the proportional controller has been applied in the flight system to

compensate for quality. The controller is based on the pitch angle θ, angle of attack α, and pitch rate q. Details are shown in Fig. 2.

$$\delta_e = K_P(\theta_c - \theta) + K_\alpha \alpha + K_q q, \tag{7}$$

where θ_c is the elevator deflections, K_P, K_α, and K_q are the control coefficients of the state feedback controller. To enable the flight system to possess a higher quality, the controller coefficients are set as K_P=−6, K_α=−5, and K_q=2.

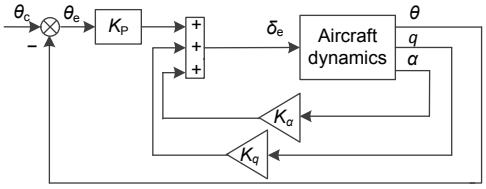

Fig. 2 Structure of the aircraft for the pitch channel

4 Results

4.1 Bifurcation analysis

The bifurcation analysis has been used to reveal all the equilibrium points of the aircraft dynamic of the longitudinal, for both SEPs and UEPs. The equilibrium points are computed by solving the differential equations and are classified by the polarity of eigenvalues. To simplify the analysis, all controller parameters are held constant, and only the elevator deflections are varied as the bifurcation parameter. The results of bifurcation diagrams for the elevator deflections from −10° to +10° are shown in Fig. 3.

Through bifurcation analysis of the diagrams, when the elevator is deflected to −2.7°, the aircraft does not have any SEPs and the aircraft system must be outside the safety envelope. With the reverse elevator increasing, the angle of attack goes up to the stall angle, and the stall elevator is at −2.2°. At the stall point, an obvious state jump can be found and it is difficult to sustain stability. A spinning motion is observed in the longitudinal channel, with the flight velocity of 116.86 m/s, the angle of attack of 20.8°, the pitch angle of −2.69°, and the pitch rate remaining at zero. To recover from the stall, the pilot must change the elevator to the safety range. Details can be found in Sieber and Krauskopf (2008). However, Sieber and Krauskopf (2008) noted only the range of a safe elevator; they did not give accurate safety boundaries for the aircraft. Even if there is a stable

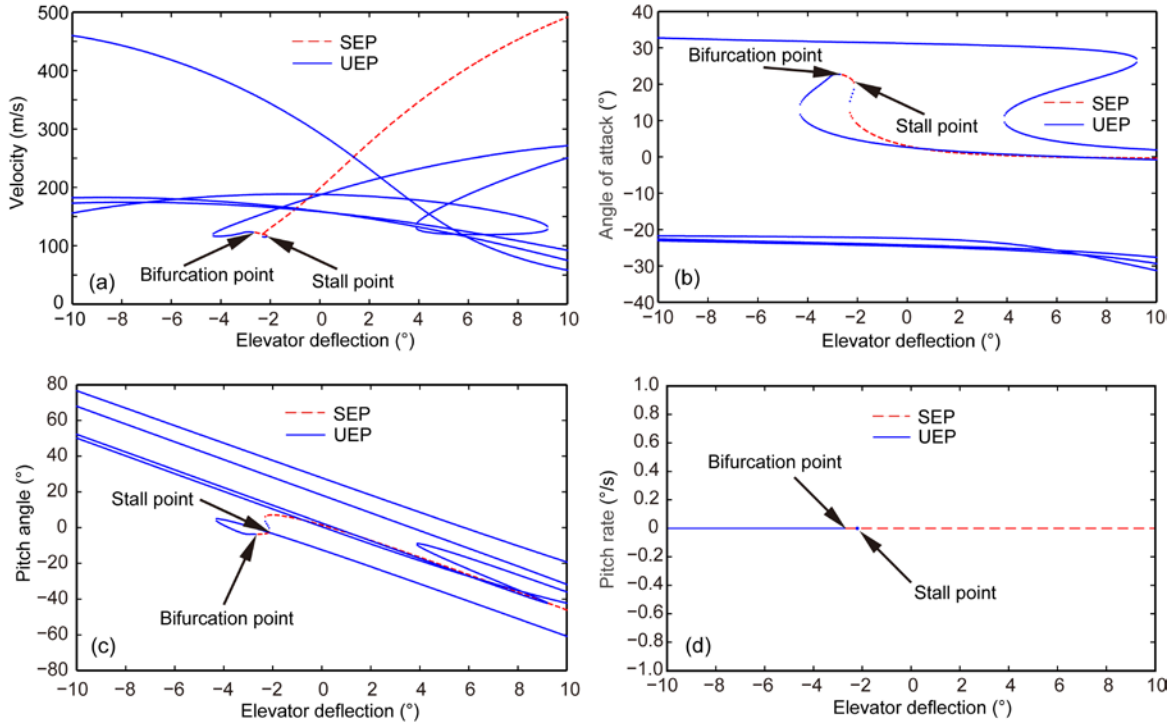

Fig. 3 Bifurcation diagrams for the velocity (a), angle of attack (b), pitch angle (c), and pitch rate (d)

SEP: stable equilibrium point; UEP: unstable equilibrium point. References to color refer to the online version of this figure

equilibrium and safety envelope, it could not ensure that the flight states are within the safety envelope. Moreover, if the safety envelope is too narrow, the flight states may easily exceed it under a disturbance due to changes of the environment. Therefore, the method to assess the flight safety envelope based on the differential manifold theory is presented.

4.2 Differential manifold theory for flight safety envelope determination

To estimate the envelope of the aircraft, the equation $f(\boldsymbol{x})=0$ should be solved first. Next, we choose all the UEPs that satisfy conditions (1)–(3) and are on the stability boundary of the SEPs of all the equilibrium points. Fig. 4 shows the trajectories of UEPs. Note that seven UEPs are obtained by calculating Eq. (1). After integration at UEPs, the trajectories of UEP1, UEP2, and UEP4 finally converge to the SEP and the trajectories of UEP3, UEP5, UEP6, and UEP7 will eventually diverge. Thus, it can be guaranteed that UEP1, UEP2, and UEP4 are the UEPs on the stable boundary.

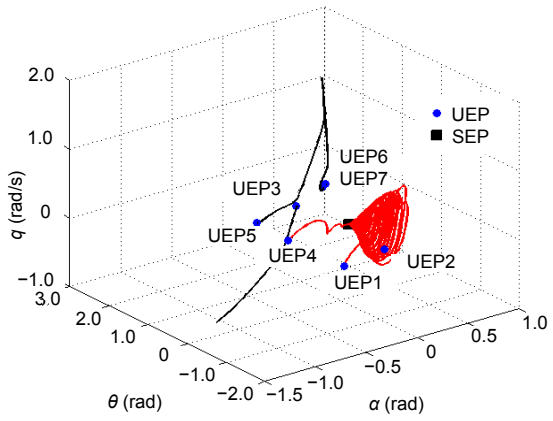

Fig. 4 Trajectories of unstable equilibrium points (UEPs)

The Monte-Carlo method has been used to verify the validity and accuracy of the stability boundary, which is determined by the differential manifold theory. This approach is shown as follows: (1) A large number of initial points are taken in the state space of the closed-loop system. (2) The trajectories are obtained by integrating the positive values at the initial point. (3) The validity and accuracy are verified by analyzing whether the convergence domain formed by the trajectory is consistent with the envelope constructed by the differential manifold theory. The Monte-Carlo method is very easy to implement. In the process of solving the trajectories, the larger the number of initial points that are taken, the higher the accuracy of the envelope. However, if too many initial points are taken, it will result in a long computation time. Therefore, the initial points must be set within an acceptable range. To make it easier for observation, the envelope determined by the Monte-Carlo method is shown in Figs. 5 and 6. Fig. 6 is a contrast map between the envelopes determined by the differential manifold method and the Monte-Carlo method. Figs. 5 and 6 show that the two methods are consistent with each other, so the validity and accuracy of the safety envelope determined by the differential manifold theory are proved.

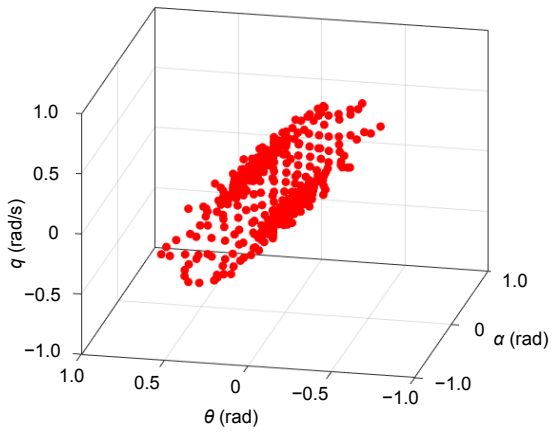

Fig. 5 Envelope under the Monte-Carlo method

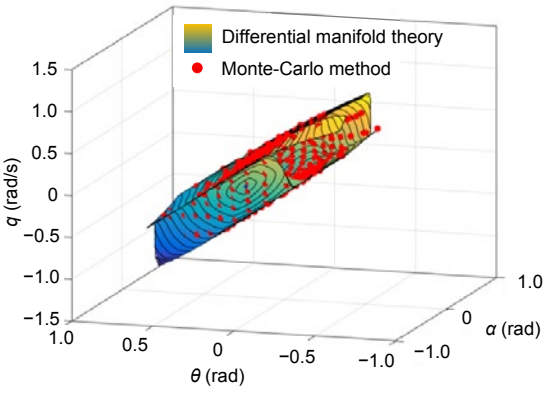

Fig. 6 Envelopes under different methods

Eq. (1) can be rewritten by Eqs. (5)–(7), where $\boldsymbol{x}$ is the vector of flight state variables. To better state the problem, the velocity is kept to 162 m/s and the trim state of the pitch rate is kept to zero. For different

elevators 0° and 10°, their equilibrium points are shown in Tables 1 and 2, respectively. X_1, X_2, X_3, Y_1, Y_2, and Y_3 are UEPs, which are on the stability boundary of X and Y, respectively.

Table 1 Equilibrium points with the elevator of 0°

Point	α (rad)	θ (rad)	q (rad/s)
X	0.0876	0.0876	0
X_1	−0.4327	0.1002	0
X_2	0.0745	−0.1435	0
X_3	0.1103	0.3175	0

Table 2 Equilibrium points with the elevator of 10°

Point	α (rad)	θ (rad)	q (rad/s)
Y	0.0857	0.026 94	0
Y_1	−0.4296	0.276 10	0
Y_2	0.0772	0.031 40	0
Y_3	0.1032	0.491 10	0

Eigenvalues of the Jacobian matrix at points X, X_1, X_2, and X_3 are as follows: λ_X: −2.6067±1.0198i, −0.4594; λ_{X_1}: −2.9377, 2.3404, −2.8859; λ_{X_2}: 10.4373, −1.0404, −0.6769; λ_{X_3}: 22.7299, −1.0652±0.5023i.

Eigenvalues of the Jacobian matrix at points Y, Y_1, Y_2, and Y_3 are as follows: λ_Y: −2.6074±1.0172i, −0.4518; λ_{Y_1}: −2.9085, 2.2827, −1.8921; λ_{Y_2}: 10.4130, −1.0452, −0.6574; λ_{Y_3}: 22.7642, −1.0665±0.5077i.

Thus, the equilibrium points show that the pitch angle in the stable state has been moved with the change of the elevator. Comparing the safety envelope based on the elevator of 0° with that based on the elevator of 10° (Fig. 7), it can be found that the envelope has been moved. To highlight the influence of the change in envelope on flight states, state point A is designed. Point A can eventually return back to the stable equilibrium while the elevator is zero, indicated by curve 1 in Fig. 7. However, for excessive forward elevator deflections, the flight state will exceed the safety boundary, indicated by curve 2. For an aircraft, if the pilot pushes the steering rod too hard, the aircraft may possibly experience LOC, even resulting in the pilot-induced oscillation.

5 Conclusions

In this study, the aims are to use the bifurcation analysis to study how the aircraft dynamic change is affected by different elevator deflections, and to determine the safety envelope based on the differential manifold theory. By using bifurcation analysis results of the research on GTM, the relationship between elevator deflections and equilibrium points has been obtained. In comparison with the Monte-Carlo method, the feasibility and accuracy of the differential manifold theory have been justified. The results showed that the bifurcation analysis method and differential manifold theory complement each other well in real time and the simultaneous use of these two methods can greatly improve the operating safety of an aircraft.

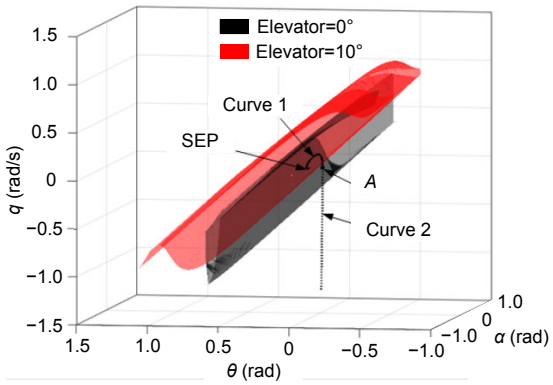

Fig. 7 Change of envelope with the pilot operation
References to color refer to the online version of this figure

Note that the controller parameters vary, which will also result in the change in the safety envelope. Moreover, for different kinds of controllers, further investigation is needed to determine the relationship between the controller parameters and the safety envelope. Furthermore, how the dynamic envelope is used in online envelope protection needs to be studied more extensively in the future.

References

Bayen AM, Mitchell IM, Oishi MK, et al., 2007. Aircraft autolander safety analysis through optimal control-based reach set computation. *J Guid Contr Dynam*, 30(1):68-77. https://doi.org/10.2514/1.21562

Chaichi M, García-Río E, Vázquez-Abal ME, 2005. Three-dimensional Lorentz manifolds admitting a parallel null vector field. *J Phys A Math Gener*, 38(4):841-850. https://doi.org/10.1088/0305-4470/38/4/005

Chiang HD, Hirsch MW, Wu FF, 1988. Stability regions of nonlinear autonomous dynamical systems. *IEEE Trans Autom Contr*, 33(1):16-27. https://doi.org/10.1109/9.357

Engelbrecht JAA, Pauck SJ, Peddle IK, 2012. Bifurcation

analysis and simulation of stall and spin recovery for large transport aircraft. AIAA Atmospheric Flight Mechanics Conf, p.1-12. https://doi.org/10.2514/6.2012-4801

Goncharova E, Ovseevich A, 2016. Small-time reachable sets of linear systems with integral control constraints: birth of the shape of a reachable set. *J Optim Theory Appl*, 168(2): 615-624. https://doi.org/10.1007/s10957-015-0754-4

Haghighatnia S, Moghaddam RK, 2013. Enlarging the guaranteed region of attraction in nonlinear systems with bounded parametric uncertainty. *J Zhejiang Univ-Sci C (Comput & Electron)*, 14(3):214-221. https://doi.org/10.1631/jzus.C1200213

Jahnke C, Culick FEC, 1994. Application of bifurcation theory to the high-angle-of-attack dynamics of the F-14. *J Aircraft*, 31(1):26-34. https://doi.org/10.2514/3.46451

Khatri AK, Sinha NK, 2011. Aircraft maneuver design using bifurcation analysis and nonlinear control techniques. 49th AIAA Aerospace Sciences Meeting Including the New Horizons Forum and Aerospace Exposition, p.1-12. https://doi.org/10.2514/6.2011-924

Khodadadi L, Samadi B, Khaloozadeh H, 2014. Estimation of region of attraction for polynomial nonlinear systems: a numerical method. *ISA Trans J Autom*, 53(1):25-32. https://doi.org/10.1016/j.isatra.2013.08.005

Klyde DH, McRuer D, 2009. Smart-cue and smart-gain concepts to alleviate loss of control. *J Guid Contr Dynam*, 32(5):1409-1417. https://doi.org/10.2514/1.43156

Krauskopf B, Osinga HM, 1999. Two-dimensional global manifolds of vector fields. *Chaos Interdiscip J Nonl Sci*, 9(3):768-774. https://doi.org/10.1063/1.166450

Krauskopf B, Osinga HM, Doedel EJ, et al., 2005. A survey of methods for computing (un)stable manifolds of vector fields. *Int J Bifurc Chaos*, 15(3):763-791. https://doi.org/10.1142/S0218127405012533

Kwatny HG, Dongmo JET, Chang BC, et al., 2013. Nonlinear analysis of aircraft loss of control. *J Guid Contr Dynam*, 36(1):149-162. https://doi.org/10.2514/1.56948

Lygeros J, Tomlin C, Sastry S, 1999. Controllers for reachability specifications for hybrid systems. *Automatica*, 35(3):349-370. https://doi.org/10.1016/S0005-1098(98)00193-9

Merret JM, Hossain KN, Bragg MB, 2002. Envelope protection and atmospheric disturbances in icing encounters. 40th AIAA Aerospace Sciences Meeting & Exhibit, p.1-18. https://doi.org/10.2514/6.2002-814

Osinga HM, 2005. Two-dimensional invariant manifolds in four-dimensional dynamical systems. *Comput Graph*, 29(2):289-297. https://doi.org/10.1016/j.cag.2004.12.016

Pandita R, Chakraborty A, Seiler P, et al., 2009. Reachability and region of attraction analysis applied to GTM dynamic flight envelope assessment. AIAA Guidance, Navigation, and Control Conf, p.1-21. https://doi.org/10.2514/6.2009-6258

Qi R, Cook D, Kliemann W, et al., 2000. Visualization of stable manifolds and multidimensional surfaces in the analysis of power system dynamics. *J Nonl Sci*, 10(2): 175-195. https://doi.org/10.1007/s003329910008

Ranter H, 2007. Airliner Accident Statistics 2006. Available from https://aviation-safety.net/pubs/asn/ASN_Airliner_Accident_Statistics_2006.pdf [Accessed on Dec. 17, 2018].

Sharma V, Voulgaris PG, Frazzoli E, 2004. Aircraft autopilot analysis and envelope protection for operation under icing conditions. *J Guid Contr Dynam*, 27(3):454-465. https://doi.org/10.2514/1.1214

Sieber J, Krauskopf B, 2008. Control based bifurcation analysis for experiments. *Nonl Dynam*, 51(3):365-377. https://doi.org/10.1007/s11071-007-9217-2

Weekly K, Tinka A, Anderson L, et al., 2014. Autonomous river navigation using the Hamilton-Jacobi framework for underactuated vehicles. *IEEE Trans Robot*, 30(5):1250-1255. https://doi.org/10.1109/TRO.2014.2327288

Xin Q, Shi ZK, 2015. Bifurcation analysis and stability design for aircraft longitudinal motion with high angle of attack. *Chin J Aeronaut*, 28(1):250-259. https://doi.org/10.1016/j.cja.2014.12.022

Zhang Y, de Vissery CC, Chu QP, 2016. Online safe flight envelope prediction for damaged aircraft: a database-driven approach. AIAA Modeling and Simulation Technologies Conf, p.1-14. https://doi.org/10.2514/6.2016-1189

Zuo ZQ, Fu YH, Chen YP, et al., 2013. A new method of reachable set estimation for time delay systems with polytopic uncertainties. *Appl Math Comput*, 221:639-647. https://doi.org/10.1016/j.amc.2013.06.099